IL NUOVO CIMENTO Vol. 31 C, N. 5-6 Settembre-Dicembre 2008
DOI 10.1393/ncc/i2009-10338-3

# Thorpe method applied to planetary boundary layer data

P. López González-Nieto(1)(*), J. L. Cano(1), D. Cano(2) and M. Tijera(1)

(1) *Departamento de Física de la Tierra, Astronomía y Astrofísica II Universidad Complutense - 28040 Madrid, Spain*

(2) *AEMET (Spanish Meteorological Agency), Ciudad Universitaria - 28040 Madrid, Spain*

(ricevuto il 30 Ottobre 2008; approvato il 30 Gennaio 2009; pubblicato online l'11 Giugno 2009)

**Summary.** — Turbulence affects the dynamics of atmospheric processes by enhancing the transport of mass, heat, humidity and pollutants. The global objective of our work is to analyze some direct turbulent descriptors which reflect the mixing processes in the atmospheric boundary layer (ABL). In this paper we present results related to the Thorpe displacements $d_T$, the maximum Thorpe displacement $(d_T)_{\max}$ and the Thorpe scale $L_T$, the Ozmidov scale and their time evolution in the ABL during a day cycle. A tethered balloon was used to obtain vertical profiles of the atmospheric physical magnitudes up to 1000 m. We discuss the vertical and horizontal variability and how different descriptors are related to atmospheric mixing.

PACS 92.60.Fm – Boundary layer structure and processes.
PACS 92.60.hk – Convection, turbulence, and diffusion.

## 1. – Introduction

Atmospheric turbulence is an important subject in the atmospheric sciences because most of the fluxes in the atmosphere depend on turbulent diffusion, especially those that generate irreversible molecular mixing. The atmospheric boundary layer (ABL) is the lower part of the atmosphere characterized by a strong interaction with the underlying surface. The ABL turbulence affects its dynamics by enhancing the physical diffusion and changing the evolution of different processes. Small-scale turbulent mixing in ABL is of great relevance for many processes ranging from medium to a local scale (air quality close to a city). Unfortunately, measuring at those small scales is very difficult. To overcome this disadvantage it is interesting to use theories and parameterizations which are based on larger scales because they are more easily accessible by conventional instruments.

(*) E-mail: azufre2@hotmail.com

 

In the absence of turbulence, atmospheric temperature profiles become increasingly monotonic, due to the smoothing effect of molecular diffusion that occurs at Bachelor/Kolmogorov scales when the 3D turbulence cascade produces molecular mixing. Turbulence at larger scales as well as other causes such as environmental instabilities or internal wave breaking (the well-known Clear Air Turbulence (CAT)) makes vertical overturns that appear as inversions in measured temperature profiles. The vertical extent of turbulent overturns can be obtained from the temperature profiles, and their study is based mainly on length scale analysis. Vertical overturns, produced by turbulence in density stratified fluids as lakes or the ABL, can often be quantified by the Thorpe displacements $d_T$, the maximum displacement length $(d_T)_{\max}$ and the Thorpe scale $L_T$.

Then, one of the aims of this work is to analyze the behaviour of overturning length scales, which can be used as a tool to infer the small-scale dynamics of turbulence from the largest overturns present in profiles. The other interest of this paper is to calculate the Thorpe displacements, the maximum Thorpe displacement and the Thorpe scale at the ABL because we want to study the properties of the ABL turbulent patches which represent one of the dominant processes for mixing. And, finally, we also want to analyze their time evolution during a day cycle in order to relate it with the ABL stratification conditions.

As mentioned before, there is a great interest to use theories and parameterizations for small-scale dynamics which are based on larger scales—as $L_T$ or $(d_T)_{\max}$. But there are also several more reasons. The correlation between $L_T$ and the Ozmidov scale $L_O$, defined below, can be used to estimate rates of dissipation of turbulent kinetic energy and vertical turbulent difussivities which describe the efficiency of turbulent mixing at small scales. So a deeper insight on this relation is helpful to estimate mixing, at least that associated with patches of high turbulent activity. Another reason is related to the theories of turbulent stirring which often depend on hypotheses about the length scales of turbulent eddies (for example, mixing length theories). And, finally, estimates of the dissipation of energy by turbulence and turbulent difussion are important for a full understanding of ABL energetic and dynamic processes. For example, turbulent mixing and diffusion of natural and anthrop-genetic gases, which are often pollutant or contribute to environmental hazards, are seen to control ABL composition both under stable and unstable conditions. Next we present the data used for the analysis, in sect. **3** we present the definitions of the scale descriptors used and finally the results are presented and discussed.

## 2. – Data sets and instrumentation

The preliminary results presented in this paper are based on ABL data from 98 balloon soundings made in Almaraz (Cáceres, Spain) with a tether balloon sensing system. The data were selected for this analysis because they cover different stratified conditions—stable, unstable and neutral—and mixing conditions—from shear-driven turbulence to convective regions.

The instrumented balloon for the ABL measurements was launched near the nuclear power station of Almaraz (CNA) from 5th to 10th June 1994 and from 25th to 29th September 1995. Almaraz (39° 45′ N, 5° 40′ W, 225 m) is located around 110 km away from Cáceres city, on the west of the Spanish plateau. Almaraz is located in the surroundings delimited by the Tiétar and Tajo rivers, which constitute a triangle-shaped environment with over eighty kilometres in the east-west axis. The longest separation between both rivers is 30 kilometres. This area is topographically influenced by the plain

Fig. 1. – Satellite view of Almaraz (Cáceres, Spain).

on the Tajo riversides and the Almaraz mountain range. The weather in this region is continental. The surroundings of the power station are constituted by pastures and meadows, as may be seen in figs. 1 and 2.

The main instrumentation used is a sounding system which includes a zeppelin-shaped tethered balloon from which a meteorological probe was hanging. The sounding balloon is joined by a fibre thread to an engine through which the up and down velocity could be regulated. Therefore, the equipment was completed by an atmospheric data acquisition system called ADAS. The ADAS received and processed the atmospheric information

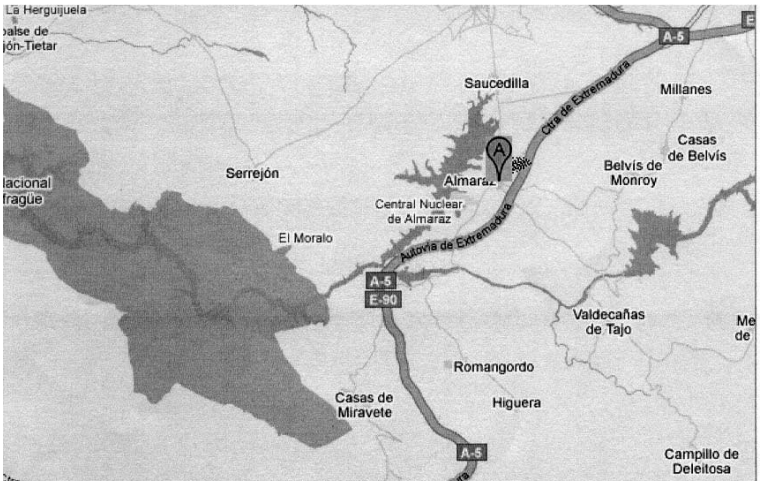


Fig. 2. – Topographic map of Almaraz (Cáceres, Spain).

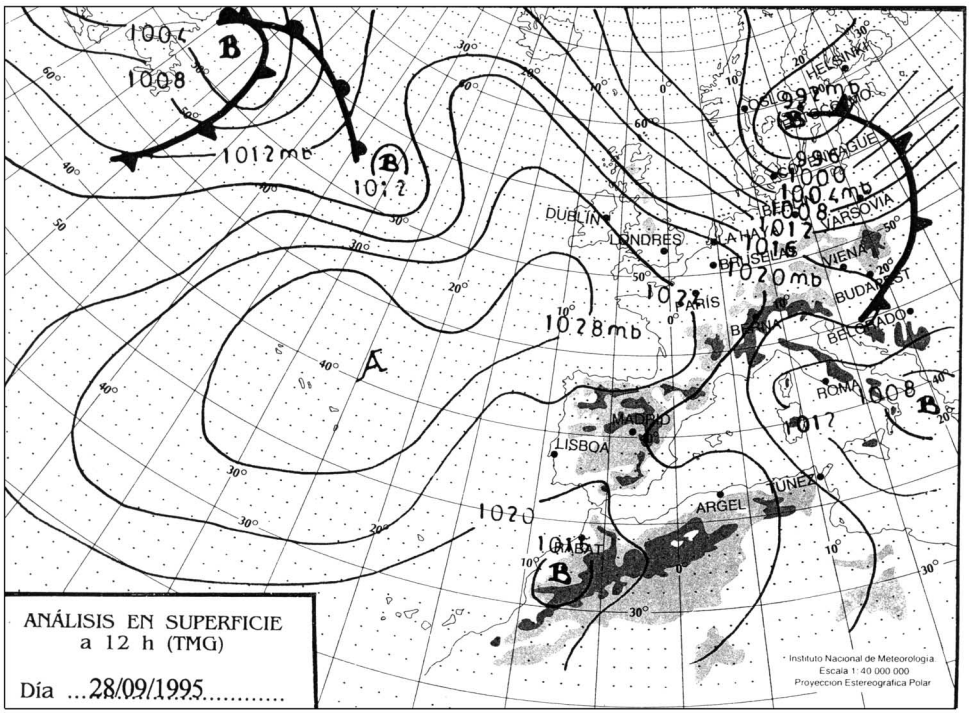


Fig. 3. – Meteorological map corresponding to 28th September 1995.

coming from probes, which transmitted the meteorological information with a sampling frequency of 403 MHz. ADAS system registered the following atmospheric data: atmospheric pressure (3 hPa of precision; 0.1 hPa of resolution), height, temperature (precision between 0.6 °C and 1 °C; 0.01 °C of resolution), time interval, wind velocity and direction.

The tethered balloon operated slowly rising at the ABL and the data acquisition can be controlled as the balloon goes up. The sampling interval of temperature, wind velocity, humidity, height and pressure data was $\Delta t = 25$ min and the vertical data resolution was about $\Delta z = 8$ m. The sampling interval of sequential profiles was about 1 h.

A total of 98 successful soundings approximately ranging from 150 m to 1000 m were carried out. We used ABL profiles obtained during balloon flights launched from 6 h to 12 h and from 15 h to 24 h in the 1995 and from 5 h to 12 h and from 17 h to 24 h in the 1994 campaigns on the above-mentioned dates. The meteorological conditions vary from clear to slightly cloudy for the 1995 campaigns whereas for the 1994 campaigns the situation consisted of slightly cloudy skies or clean skies with cloudy intervals. As an example, fig. 3 shows the meteorological situation corresponding to 28th September 1995.

## 3. – Thorpe method

Turbulence produces vertical overturns that appear as inversions in measured temperature profiles, as mentioned before. Thorpe devised an objective technique for evaluating a vertical length scale associated with overturns in a stratified flow [1]. Thorpe's method is commonly used in oceanic and lake measurements, also in laboratory experiments (for

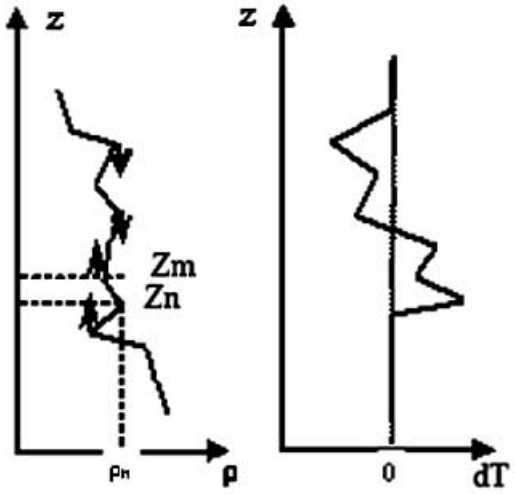


Fig. 4. – Scheme of a distinguishable overturn as well as the corresponding Thorpe displacements with their characteristic $\boldsymbol{Z}$ pattern.

example, study of the vertical overturns occurring behind a biplane grid in a continuously stratified water channel [2]), and in the tropo-stratosphere to analyze turbulent parameters [3], but has never been applied to ABL measurements.

For horizontally homogeneous flows, Thorpe's technique evaluates a vertical length scale associated with overturns in a stratified flow as follows [1]. If one considers an instantaneous vertical density profile $\rho(z)$, as the left graph of fig. 4 shows, part of this profile appears to contain inversions which are gravitationally unstable. Thorpe's technique consists of rearranging this density profile $\rho(z)$ so that each fluid particle is statically stable. The result of the method is a stable monotonic profile which contains no inversions. Imagine a density profile as consisting of $i$ samples of density $\rho_i$, each of which was observed at depth $z_i$. If the sample at depth $z_n$ must be moved to depth $z_m$ to generate the stable profile, the Thorpe displacement $d_T$ is $z_m - z_n$ (fig. 4). The distances $d_T(z)$ each fluid particles have been displaced are shown in fig. 4, right graph, and are called Thorpe displacements. As turbulent eddies are not one-dimensional, the displacement $d_T$ is not necessarily the distance sample actually travelled [1, 4].

The Thorpe displacements let us to define overturns as a profile section for which $\sum_i d_{T_i} = 0$ while $d_{T_i} \neq 0$ for most $i$ [4, 5].

Two Thorpe scales can be defined from the root mean square (r.m.s.) and the maximum of the Thorpe displacements, respectively, as [1], [2], and [4]:

$$(L_T)_{\text{r.m.s.}} = \left\langle d_T^2(z) \right\rangle^{1/2} \rightarrow \textit{Thorpe scale}, L_T \tag{1}$$

and

$$(L_T)_{\max} = \max[d_T(z)] \rightarrow \textit{Maximum Thorpe Displacement}, \tag{2}$$

where $\langle\ \rangle$ signifies an appropriate averaging process. The scale $(L_T)_{\text{r.m.s.}} = L_T$ characterizes the turbulent motion at the time of the measurements and it is a statistical

measure of the vertical size of overturning eddies [4, 6]. The scale $(L_T)_{\max}$ represents the larger overturns which might have occurred at an earlier time when buoyancy effects were negligible [2] and, in some cases, is considered as an appropriated measure of the overturning scale.

By setting the buoyancy forces equal to the inertial forces, Ozmidov [7] derived a length scale $L_O$ which would describe the largest possible overturning turbulent scale allowed by buoyancy as

$$L_O = \sqrt{\frac{\varepsilon}{N^3}}, \tag{3}$$

where $\varepsilon$ is the kinetic energy dissipation rate and $N$ the Brunt-Väisälä frequency. This relation is helpful to estimate mixing, at least that associated with patches of high turbulent activity [6]. Various measurements have shown that the Thorpe scale is nearly equal to the energy containing length scale or Ozmidov scale, $L_O$. For example, far from the surface in wind-forced mixing layers in the seasonal thermocline the overall relationship $\langle L_T/L_O \rangle = 1.25$ has been reported [4]. Other results present a wider range: $\langle L_T/L_O \rangle = [0.9, 1.4]$ for measurements of turbulence during conditions of wear overflow [4-6, 8]. This is very important because it can be used to calculate the dissipation rate $\varepsilon$ from $L_T$ and the stability $N^2$ using the definition of the Ozmidov length scale. Therefore, the Thorpe scales can be used to estimate rates of dissipation of turbulent kinetic energy and this is an essential result. Moreover, the length scale ratio $L_T/L_O$ can be interpreted as a "clock", which increases monotonically as the turbulent event evolves [6, 9]. The ratio changes from values less than 0.5 for recent, relatively low Reynolds numbers turbulent overturns to about 1 after the transition to turbulence and increases beyond 1 as turbulence finally decays.

## 4. – Results

Our methodology used potential temperature instead of density and is based on reordering 98 measured potential temperature profiles, which may contain inversions, to the corresponding stable monotonic profiles. Then, the profiles of the displacement length scales $d_T(z)$ can be calculated. Each displacement $d_T$ represents the vertical distance that each measured potential temperature value has to move up- or downward to its position in the stable monotonic profile. To get the Thorpe displacements profiles, a bubble sort algorithm with ordering beginning at the lowest depth was used in the analysis [1], [2] and [4].

Figures 5 to 7 show the time evolution of the potential temperature, the potential temperature fluctuations, the vertical potential temperature gradient and the Thorpe displacements profiles from 07 GMT (at sunrise) to 24 GMT. Thorpe displacements are useful as a visual aid to define the vertical extent of some mixing events.

Thorpe displacements observed at profiles could be qualitative classified in two groups: isolated $Z$ patterns corresponding to discrete patches and distributed and indistinct features. The isolated overturns are very few well-defined sharp overturns and they appear under stability conditions (at sunset, night and sunrise profiles). The non-zero Thorpe displacement regions with indistinct features appear under convective and/or neutral conditions (at noon, afternoon and evening profiles) and are smaller.

Usually, the signature which might be expected for a large overturning eddy is: sharp upper and lower boundaries with intense mixing inside—displacement fluctuations of

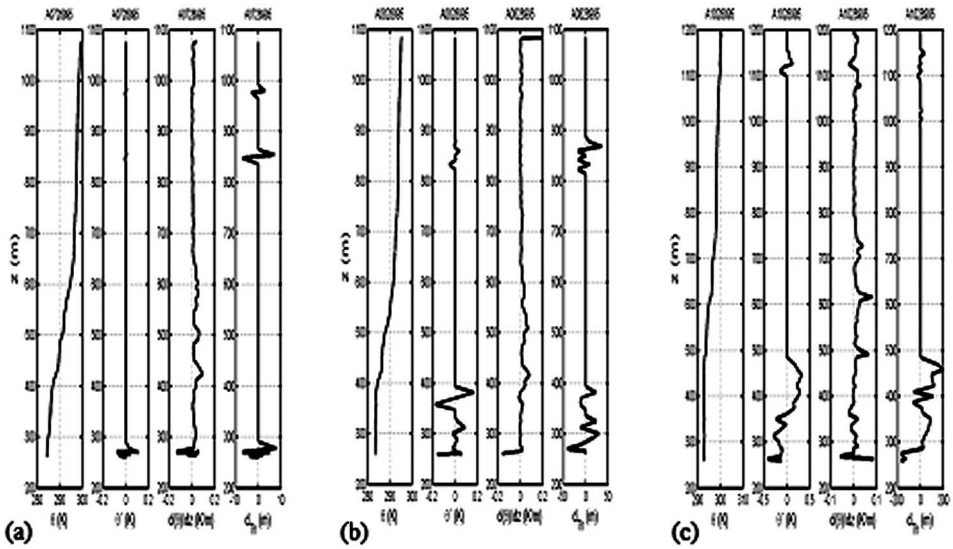


Fig. 5. – From left to right, each graph shows the potential temperature, the potential temperature fluctuations, the vertical temperature gradient and the Thorpe displacements profiles. (a) At 07 GMT (approximately at sunrise). (b) At 08 GMT. (c) At 10 GMT.

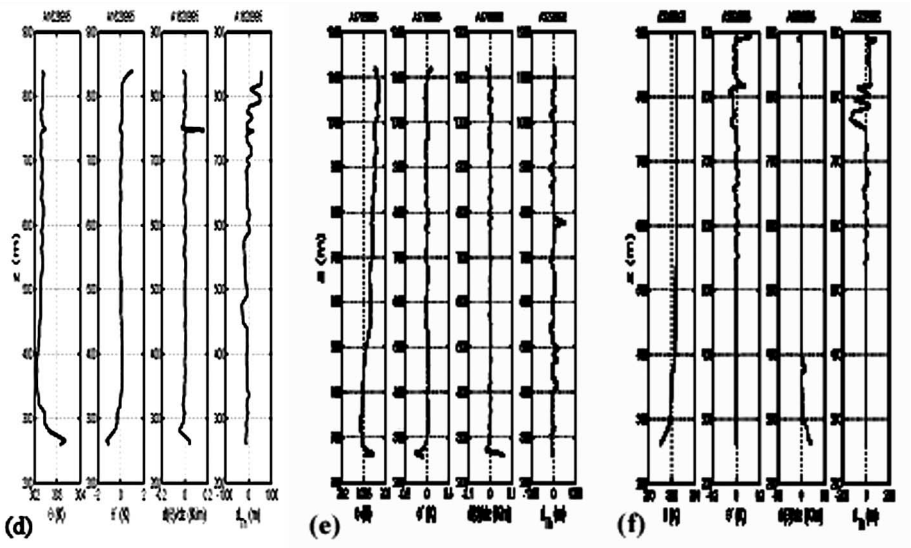


Fig. 6. – From left to right, the potential temperature, the potential temperature fluctuations, the vertical temperature gradient and the Thorpe displacements profiles. (d) At 16 GMT. (e) At 17 GMT. (f) At 20 GMT (approximately at sunset).

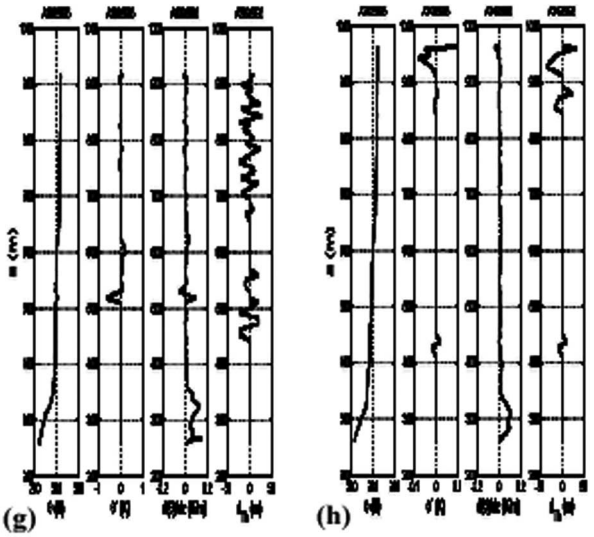


Fig. 7. – From left to right, each graph shows the potential temperature, the potential temperature fluctuations, the vertical temperature gradient and the Thorpe displacements profiles. (g) At 23 GMT. (h) At 24 GMT.

a size comparable to the size of the disturbance itself are found in the interior. While common in surface layers strongly forced by the wind, these large features are not always found as in our ABL case. We really find other features that are smaller, some having an eddylike shape similar to the larger disturbances, some a random mix of small-scale fluctuations without sharp boundaries.

In sect. **3** we have defined the Thorpe scale as

$$(L_T)_{\text{r.m.s.}} = \left\langle d_T^2(z) \right\rangle^{1/2}, \tag{4}$$

where $\langle\ \rangle$ has been chosen as a vertical average over a region of constant potential temperature gradient (the absolute value of the gradient is less than 10% of the maximum temperature gradient [2]). The Thorpe scale is proportional to the mean eddy size as long as the mean horizontal potential temperature gradient is much smaller than the vertical gradient as happens at the ABL. Figure 8 shows the time evolution of the maximum Thorpe displacement, $(d_T)_{\max}$, and the Thorpe scale, $L_T$.

The scale $(d_T)_{\max}$, or maximum Thorpe displacement, is approximately zero under stability conditions (between sunset and sunrise); it reaches a minimum region at noon under convective conditions and it reaches a maximum in the evening hours under convective/neutral conditions. We can observe that the scale $(d_T)_{\max}$ has always negative values when it is not approximately zero and it is only positive in the evening hours—from 18:00 to 24:00.

The Thorpe scale $L_T$ is approximately zero under stability conditions (between sunset and sunrise); it reaches a clear maximum under convective conditions at noon and a secondary maximum in the afternoon hours under convective to neutral conditions.

Then, we observe that the Thorpe scale $L_T$ reaches its maximum values—at 11:00 a.m.—approximately at the same time interval as $(d_T)_{\max}$ reaches its minimum values—

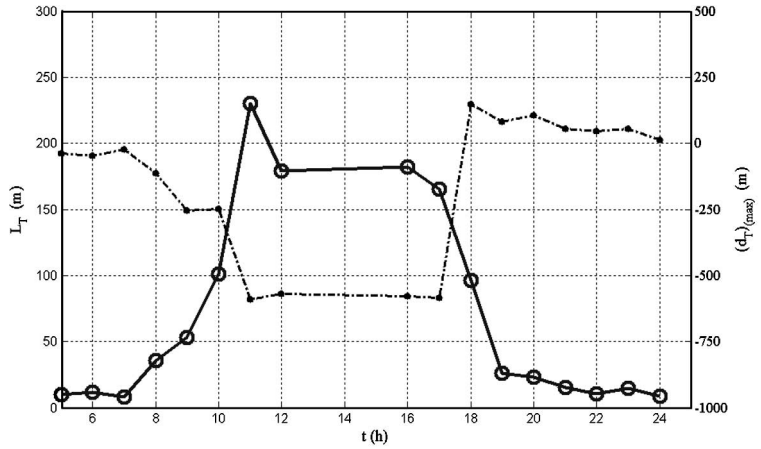


Fig. 8. – The dotted curve shows the time evolution of the maximum of Thorpe displacements, $(d_T)_{\max}$. The continuous curve is the Thorpe scale time evolution.

from 11:00 to 17:00. Then, there are two distinct behaviours with high ($L_T > 150\,\mathrm{m}$) and low ($L_T < 10\,\mathrm{m}$) magnitudes of the Thorpe scales. We propose that in most of the patches in inner layers the Thorpe scale does not exceed several meters and they appear under stable and neutral conditions when the Thorpe displacements are related to instantaneous density gradients. In contrast, under convective conditions, Thorpe scales are relatively large and may be related to convective burst.

Both scales, $L_T$ and $(d_T)_{\max}$, are close to zero at sunset, midnight and sunrise. Moreover, the Thorpe scale is always positive, or approximately zero, during the day cycle, but the maximum Thorpe displacement is always negative except at evening (from 18:00 to 24:00).

As mentioned before, the maximum Thorpe displacement can be considered as an appropiated measure of the overturning scale. Other researchers have found a linear relationship between $L_T$ and $(d_T)_{\max}$ for profiles from the equatorial undercurrent [5,8]. For microstructure profiles from lakes under very different conditions of mixing and stratification, a power law—as $(d_T)_{\max} \sim (L_T)^{0.85}$—is found [10,11]. Figure 9 shows a graph which represents that for the ABL data we observe a linear relation between these two scales, $L_T$ and $(d_T)_{\max}$ with a correlation coefficient $r^2 = 0.92$.

In the future, we will choose to use the Thorpe scale rather than the maximum displacement because we only sample vertically while the turbulence is three dimensional and, therefore, the Thorpe scale or r.m.s. displacement is more likely to be a statistically stable representation of the entire feature. This is important because we have to choose an appropiated overturning scale to make a comparison with the Ozmidov scale at ABL data [4,6,11].

Other descriptors may also be compared with the Thorpe scale, such as an equivalent atmospheric scale to the Cox scale used in oceanography, or the typical vertical distanced travelled by the fluid particles before either returning to their equilibrium or mixing [12], calculated from density or temperature as

$$L_t = \rho'/(\mathrm{d}\rho/\mathrm{d}z), \tag{5}$$

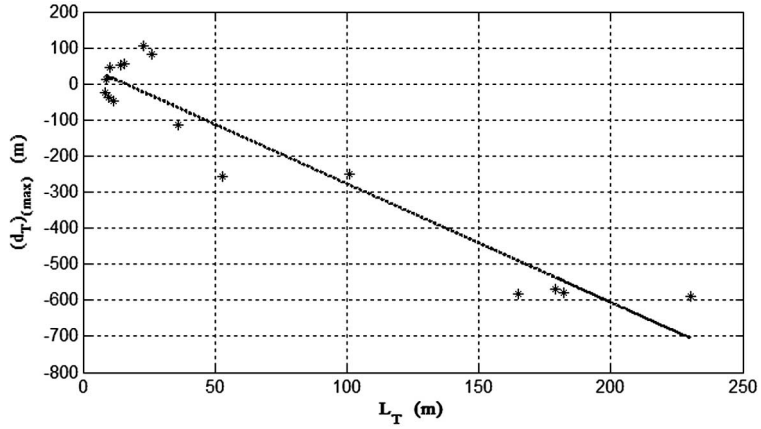


Fig. 9. – The maximum of Thorpe displacements, $(d_T)_{\max}$ *vs.* the Thorpe scale $L_T$. The corresponding linear adjustment is shown: $(d_T)_{\max} = -3.2923\ L_T + 52.515$ with a correlation coefficient $r^2 = 0.9157$.

or the Monin-Obukhov scale:

$$L_{MO} = {u_*}^3\ T/g\kappa\langle w'T'\rangle. \tag{6}$$

It is often assumed that there is a linear relationship between $L_T$ and $L_t$, but this is not often the case and then other parameters such as the Mixedness [13] are needed. The complex interaction between the different length-scales in a stable ABL will probably set some limits to the forcing intermittent behaviour detected by [14,15] as well as producing some non-linear coupling between scales depending on the actual interaction between the forcing and the turbulent cascade.

The probability distribution of Thorpe scales was analyzed using the estimates of $L_T$. The empirical probability of Thorpe scale follows approximately the exponential model, which assumes the highest probability for very small amplitudes of $L_T$ (fig. 10, on the left). The Weibull plot and the exponential plot for the Thorpe scales are shown in fig. 10, on the right. They are plots that help determine if the data can be reasonably modeled using a Weibull distribution or an exponential distribution. If the data come from a Weibull or an exponential distribution, the points will lie approximately along the corresponding straight line (a reference line is superimposed on each plot). Figure 10, on the right, shows that the points are closer to the line of the exponential model. Other researchers have suggested that exponential distribution can serve as a good approximation for the Thorpe scale, at least in aquatic environments at lakes [11]. This hypothesis is approximately confirmed by our results shown in fig. 10. Therefore, the empirical probability distribution of Thorpe scales follows an exponential model. This model could be used for $L_T$ distribution where turbulence is highly intermittent and generally weak, but it is not relevant for active turbulent regions such as permanent wind-induced turbulent zones where mixing generates turbulent eddies of the sizes proportional to $L_T$ (probability of very small $L_T$ is low) [16]. The Weibull distribution can serve as an alternative of the exponential model for the Thorpe scales from active turbulent regions and Weibull distribution can be used to model pdf of vertical density gradients [16]. But we observe that our results do not accurately adjust to the Weibull distribution, and one of the reasons may be the effect of intermittency (right graph of fig. 10).

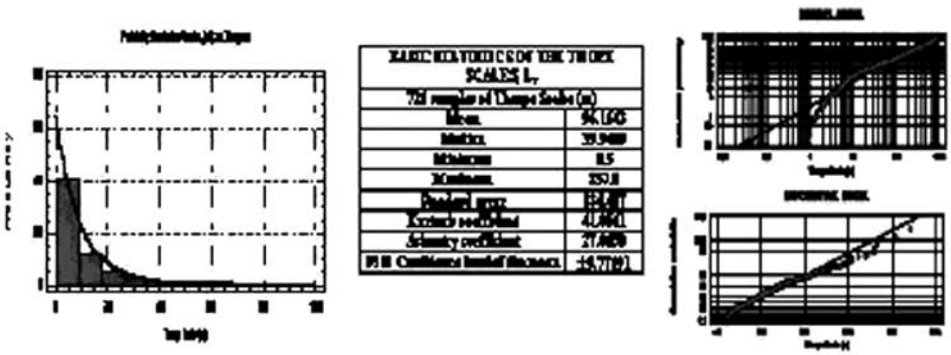

Fig. 10. – On the left, the frequency histogram and the exponential distribution curve shown as an overlay corresponding to Thorpe scales. In the middle, basic statistics of the measured Thorpe scales. On the right, the two probability distributions used to analyze the Thorpe scales behaviour.

The assumption that the Thorpe scales have a universal probability distribution can be used to verify how accurately the Thorpe scales were computed. It is very likely that the distribution itself or its parameters depend on the governing background conditions generating Thorpe displacements, which are different in the boundary layers from those in the interior layers with intermittent mixing, such measurements of the intermittency of the forcing, as well as that of the actual scale to scale stratified turbulence cascade are discussed in [14, 15, 17] and may be a combination of the boundary condition effects and of stability combining the 3D and 2D characteristics of scale to scale direct and inverse cascades.

## 5. – Conclusions

This paper presents some preliminary results related to the time evolutions of the ABL turbulent parameters $d_T$, $L_T$, and $(d_T)_{\max}$ during a day cycle, regarding different levels of stabilty/unstability and the turbulence developed during a day. The main conclusions from this study are as follows.

Thorpe displacements observed at profiles could be qualitative classified in two groups: isolated $Z$ patterns corresponding to discrete patches of identified overturns and the non-zero Thorpe displacement regions with indistinct features. The isolated overturns appear under stability conditions (at sunset, night and sunrise profiles). The distributed and indistinct features appear under convective and/or neutral conditions (at noon, afternoon and evening profiles). As a consequence, in the future, we will study Thorpe displacement profiles corresponding to ABL data in stable conditions. For this purpose, we will use a set of afmotpheric data from SABLES2006 field campaign which took place from 19th June to 2nd July 2006 at the CIBA site (Valladolid, Spain). We will intend to analyze only stable situations (using nocturnal ABL profiles collected at SABLES2006) because our goal is to study Thorpe displacement associated to shear-driven overturns.

We can observe that the scales $L_T$ and $(d_T)_{\max}$ have an opposite behaviour under convective conditions—between 11:00 and 17:00—because the Thorpe scale reaches a maximum at 11:00 and the maximum Thorpe displacement reaches a minimum at the same time—in fact, there appears a minimum zone between 11:00 and 17:00. Moreover,

the Thorpe scale is always positive (or approximately zero), during the day cycle, but the maximum Thorpe displacement is always negative except in the evening (from 18:00 to 24:00). Finally, both scales are close to zero at sunset, midnight and sunrise. The varying height of the well-mixed layer and the interaction of boundary layer roughness with the stratification is also directly related with the local entrainment as discussed by [18], terrain shape can interact with the ability of the ABL to produce local mixing very near the ground, this will need further field work where different conditions are met. For example the location of mixing events in a 3 or 4 dimensional parameter space formed by ($L_O$, $L_T$, $L_{MO}$, $L_t$). The relation between the Thorpe scale $L_T$ and the Ozmidov scale $L_O$ is very interesting because if the Thorpe scale is nearly equal to the energy containing length scale, then the scale $L_T$ can be used to estimate rates of dissipation of turbulent kinetic energy $\varepsilon$ using the definition of the Ozmidov length scale. These are the reasons why this relation will be studied in future research works for atmospheric data sets collected at the ABL.

* * *

We acknowledge the help of Profs. M. Velarde and A. M. Tarquis and the facilities offered by the Pluri-Disciplinary Institute of the Complutense University of Madrid. Thanks are also due to ERCOFTAC (SIG 14) and the AEMET for funding part of this research.

REFERENCES

[1] Thorpe S. A., *Philos. Trans. R. Soc. London, Ser. A*, **286** (1977) 125.
[2] Itsweire E. C., *Phys. Fluids*, **27** (1984) 764.
[3] Gavrilov N. M., Luce H., Crochet M., Dalaudier F. and Fukao S., *Ann. Geophys.*, **23** (2005) 2401.
[4] Dillon T. M., *J. Geophys. Res.*, **87** (1982) 9601.
[5] Peters H., Gregg M. C. and Sanford T. B., *J. Geophys. Res.*, **100** (1995) 18349.
[6] Fer I., Skogseth R. and Haugan P. M., *J. Geophys. Res.*, **109** (C01005) (2004) 1.
[7] Ozmidov R. V., *Atmos. Ocean. Phys.*, **8** (1965) 853.
[8] Moum J. N., *J. Geophys. Res.*, **101** (1996) 14095.
[9] Smyth W. D. and Moum J. N., *Phys. Fluids*, **12** (2000) 1327.
[10] Galbraith P. S. and Kelley D. E., *J. Atmos. Ocean. Tech.*, **13** (1996) 688.
[11] Lorke A. and Wüest A., *J. Geophys. Res.*, **107** (2002) 7-1.
[12] Redondo J. M. and Cantalapiedra I. R., *Appl. Sci. Res.*, **51** (1993) 217.
[13] Redondo J. M. and Metais O., *Mixing in Geophysical Flows* (CIMNE, Barcelona) 1995, p. 415.
[14] Vindel J. M., Yagüe C. and Redondo J. M., *Non Linear Proc. Geophys.*, **15** (2008) 915.
[15] Vindel J. M., Yagüe C. and Redondo J. M., these proceedings.
[16] Roget E., Lozovatsky I., Sánchez X. and Figueroa M., *Prog. Ocean.*, **70** (2006) 126.
[17] Yagüe C., Viana S., Maqueda G. and Redondo J. M., *Non Linear Proc. Geophys.*, **13** (2006) 185.
[18] Redondo J. M., *J. Hazardous Mater.*, **16** (1987) 381.